Project: **832**

Project title: **Cloud-resolving modeling of contrails and cirrus**

Principal investigator: **Simon Unterstrasser**

Report period: **2024-11-01 to 2025-10-31**

Maximum of 2 pages including figures. 9 pt minimum font size.

INTRODUCTION

We employ the LES model EULAG-LCM for simulations of naturally forming cirrus and for aircraft induced cirrus, so-called contrail-cirrus. The microphysical module LCM uses Lagrangian particles to transport the ice crystals and calculate the microphysical processes along their trajectories (Sölch & Kärcher, 2010). The simulations can be grouped into three categories: Simulations of contrail formation (first few seconds), young contrails (age < 5min), and simulations of contrail-cirrus and natural cirrus (time scale of hours).

SIMULATION ACTIVITIES

H2CONTRAIL-VP-REVIEW

The simulation work for this block was completed this year. It deals with high-resolution simulations of young contrails during the vortex phase (VP), which is characterised by an interplay of ice microphysics and wake vortex dynamics. For typical kerosene combustion, contrail ice crystals form on emitted soot particles (Bier et al, 2022). Hydrogen combustion is a promising technological mitigation option of the aviation's climate impact. When burning hydrogen (H2), no soot particles are emitted and fewer ice crystals form on entrained ambient aerosol particles (Bier et al, 2024). In a comprehensive modelling study, the sensitivity of the subsequent contrail evolution during the vortex phase to the initial ice crystal number was examined. For a large set of meteorological conditions and two different aircraft types, simulations with different initial ice crystal numbers were performed (factor 10 and 100 up and down relative to a typical "kerosene" contrail). In recent years, reviewers of our proposals were often concerned about a lack of justification of the manifold sensitivity studies. The following table is extracted from the paper (Lottermoser & Unterstrasser, 2025a) and lists 150 simulations (each needs resources of 40 to 80 Nh) that were all performed inside the H2CONTRAIL-VP block over the last years. The different columns show the set of setup parameters (see top row) that have been varied: the aircraft (AC) type, ambient temperature T_{amb}, relative humidity $RH_{i,amb}$, Brunt-Väisälä frequency N_{BV}, initial number of ice crystals N_0, amount of emitted water vapour I_0 and the width of the ice crystal size distribution r_{SD}. It is clearly out of scope to explain the motivation behind each simulation here. Moreover, additional simulations for grid sensitivity studies, further parameter variations (like ambient pressure) and for testing are not listed.

Table A1. Summary of the simulations performed. Columns 3–5 list the meteorological parameters, while columns 6–8 present the microphysical initializat
10 display both the simulated and parameterized survival fractions. Lastly, columns 11–13 specify the length scales employed in the parameterization. Row:
correspond to sets with N_0-scaling factors of 100, 10, 1, 0.1, and 0.01. Rows showing three simulations represent sets with scaling factors of 100, 1, and 0.0
six simulations are included, with simulation 11 using a scaling factor of 1000.

No.	AC	T_{CA} (K)	$RH_{i,amb}$ (%)	N_{BV} ($10^{-2}\,s^{-1}$)	N_0 #sim	I_0 ($g\,m^{-1}$)	r_{SD}	$f_{N,s}$	$\hat{f}_{N,s}$	z_{atm} (m)	z_{emit} (m)	$\hat{z}_{desc}$ (m)
1, 2, 3, 4, 5	A350	217	120	1.15	5	15.0	3.0	0.05, 0.23, 0.65, 0.89, 0.98	0.06, 0.23, 0.6, 0.87, 0.97	164	249	339
6,7,8,9,10	A350	217	110	1.15	5	15.0	3.0	0.02, 0.1, 0.28, 0.46, 0.71	0.0, 0.06, 0.22, 0.58, 0.86	85	249	339
11, 12, 13, 14, 15, 16	A350	217	120	1.15	6	38.55	3.0	0.02, 0.09, 0.39, 0.85, 0.98, 1.0	0.05, 0.2, 0.57, 0.85, 0.96, 1.0	164	546	339
17, 18, 19, 20, 21	A350	217	110	1.15	5	38.55	3.0	0.07, 0.27, 0.63, 0.81, 0.92	0.08, 0.29, 0.68, 0.9, 0.98	85	546	339
22, 23, 24	A350	217	120	1.15	3	15.0	1.0	0.07, 0.88, 1.0	0.06, 0.6, 0.97	164	249	339
25, 26, 27	A350	217	120	1.15	3	15.0	4.0	0.05, 0.61, 0.98	0.06, 0.6, 0.97	164	249	339
28, 29, 30	A350	217	110	1.15	3	15.0	1.0	0.05, 0.49, 0.93	0.0, 0.21, 0.86*	85	249	339
31, 32, 33	A350	217	110	1.15	3	15.0	4.0	0.02, 0.26, 0.67	0.0, 0.22, 0.86	85	249	339
34, 35, 36	A350	217	120	1.15	3	38.55	1.0	0.18, 1.0, 1.0	0.2, 0.85, 1.0	164	546	339
37, 38, 39	A350	217	120	1.15	3	38.55	4.0	0.09, 0.81, 0.99	0.2, 0.85, 1.0	164	546	339
40, 41, 42	A350	217	110	1.15	3	38.55	1.0	0.18, 0.92, 1.0	0.08, 0.68, 0.98	85	546	339
43, 44, 45	A350	217	110	1.15	3	38.55	4.0	0.06, 0.58, 0.89	0.08, 0.68, 0.98	85	546	339
46, 47, 48	A350	217	120	0.5	3	15.0	3.0	0.02, 0.28, 0.66	0.0, 0.26, 0.94	164	249	515
49, 50, 51	A350	217	110	0.5	3	15.0	3.0	0.01, 0.1, 0.31	0.0, 0.02, 0.73	85	249	515
52, 53, 54	A350	217	120	0.5	3	38.55	3.0	0.04, 0.46, 0.84	0.02, 0.71, 1.0	164	546	515
55, 56, 57	A350	217	110	0.5	3	38.55	3.0	0.02, 0.26, 0.53	0.0, 0.36, 0.96	85	546	515
Simulations at higher ambient temperatures												
58, 59, 60, 61, 62	A350	225	120	1.15	5	15.0	3.0	0.02, 0.12, 0.45, 0.76, 0.95	0.03, 0.14, 0.44, 0.79, 0.94	177	110	339
63, 64, 65, 66, 67	A350	225	110	1.15	5	15.0	3.0	0.01, 0.04, 0.13, 0.25, 0.45	0.0, 0.01, 0.09, 0.3, 0.69	92	110	339
68, 69, 70, 71, 72	A350	225	120	1.15	5	38.55	3.0	0.04, 0.21, 0.63, 0.9, 0.99	0.08, 0.28, 0.67, 0.9, 0.98	177	262	339
73, 74, 75, 76, 77	A350	225	110	1.15	5	38.55	3.0	0.02, 0.1, 0.29, 0.46, 0.68	0.0, 0.07, 0.27, 0.65, 0.89	92	262	339
78, 79, 80, 81, 82	A350	230	120	1.15	5	38.55	3.0	0.03, 0.15, 0.51, 0.83, 0.97	0.05, 0.21, 0.57, 0.86, 0.97	186	163	339
83, 84, 85, 86, 87	A350	230	110	1.15	5	38.55	3.0	0.01, 0.05, 0.17, 0.31, 0.52	0.0, 0.03, 0.15, 0.46, 0.81	97	163	339
88, 89, 90, 91, 92	A350	233	120	1.15	5	38.55	3.0	0.02, 0.12, 0.45, 0.78, 0.97	0.05, 0.19, 0.53, 0.84, 0.96	191	123	339
93, 94, 95, 96, 97	A350	233	110	1.15	5	38.55	3.0	0.01, 0.04, 0.14, 0.26, 0.45	0.0, 0.02, 0.12, 0.38, 0.76	99	123	339
98, 99, 100	A350	233	120	1.15	3	38.55	1.0	0.03, 0.63, 1.0	0.04, 0.53, 0.96*	191	123	339
101, 102, 103	A350	233	120	1.15	3	38.55	4.0	0.02, 0.43, 0.96	0.05, 0.53, 0.96	191	123	339
104, 105, 106	A350	233	110	1.15	3	38.55	1.0	0.01, 0.25, 0.59	0.0, 0.12, 0.76	99	123	339
107, 108, 109	A350	233	110	1.15	3	38.55	4.0	0.01, 0.12, 0.43	0.0, 0.12, 0.76	99	123	339
110, 111, 112, 113, 114	A350	235	120	1.15	5	38.55	3.0	0.02, 0.11, 0.43, 0.75, 0.95	0.04, 0.18, 0.52, 0.83, 0.96	195	102	339
115, 116, 117, 118, 119	A350	235	110	1.15	5	38.55	3.0	0.01, 0.03, 0.12, 0.23, 0.42	0.0, 0.01, 0.1, 0.34, 0.73	101	102	339
Simulations with A320/B737-like aircraft												
120	A320	217	120	1.15	1	3.7	3.0	0.89	0.72	164	176	231
121, 122, 123	A320	225	120	1.15	3	3.7	3.0	0.05, 0.78, 1.0	0.13, 0.64, 0.96	177	76	231
124, 125, 126	A320	225	110	1.15	3	3.7	3.0	0.01, 0.29, 0.86	0.03, 0.21, 0.78	92	76	231
127, 128, 129	A320	225	120	1.15	3	9.51	3.0	0.07, 0.85, 1.0	0.2, 0.76, 0.99	177	185	231
130, 131, 132	A320	225	110	1.15	3	9.51	3.0	0.03, 0.52, 0.96	0.07, 0.39, 0.9	92	185	231
133, 134, 135	A320	230	120	1.15	3	9.51	3.0	0.05, 0.8, 1.0	0.17, 0.72, 0.98	186	114	231
136, 137, 138	A320	230	120	1.15	3	9.51	3.0	0.02, 0.35, 0.88	0.04, 0.29, 0.85	186	114	231
139, 140, 141	A320	233	120	1.15	3	9.51	3.0	0.04, 0.78, 1.0	0.16, 0.71, 0.97	191	85	231
142, 143, 144	A320	233	110	1.15	3	9.51	3.0	0.01, 0.3, 0.86	0.04, 0.26, 0.82	99	85	231
145, 146, 147	A320	235	120	1.15	3	9.51	3.0	0.04, 0.76, 1.0	0.16, 0.7, 0.97	195	70	231
148, 149, 150	A320	235	110	1.15	3	9.51	3.0	0.01, 0.27, 0.84	0.03, 0.24, 0.81	101	70	231

Figure 1: List of systematic parameter variations (150 simulations) analysed in publication by Lottermoser und Unterstrasser (2025a). Not listed are additional parameter variations (like ambient pressure), grid sensitivity studies nor test simulations.

One crucial process during the vortex phase is the partial loss of ice crystals (due to adiabatic heating in the descending wake vortices with ice trapped inside) and the simulations are used to quantify the ice crystal survival fraction f_{Ns} (the fraction of the ice crystal that is not lost during the vortex phase). Unterstrasser (2016) designed an analytical parametrisation of f_{Ns} as a function of the aforementioned parameters. In the meantime, this parametrisation has been implemented in the ECHAM GCM for a refined contrail initialisation and an updated contrail radiative forcing estimate (Bier & Burkhardt, 2022). Based on the extended set of new simulations, in particular in the high temperature range ($T_{amb} \geq 225K$) and for a large N_0 variation, an updated version of the f_{Ns} parametrisation has currently already been implemented in ECHAM. This enables robust estimates of the H2 contrail radiative forcing.

H2CONTRAIL-DP

The block called "H2CONTRAIL-DP" deals with high-resolution dispersion phase (DP) simulations of aging contrail-cirrus. With such simulations, changes in climate-relevant contrail-cirrus properties are evaluated and its dependence on the initial ice crystal number is explored. Those simulations use the simulation data from **H2CONTRAIL-VP** as initialization. In addtion to the parameters listed above, the synopic evolution of ambient temperature and RH_i ("updraught scenarios") serve as additional degrees of freedom in the simulation setup. In total, around 300 further simulations have been performed (each simulation needs 4 to 8 Nh). The simulation work is finished and the results are the basis of a manuscript that is currently under review (Lottermoser & Unterstrasser, 2025b). As a spin-off, a subset of these simulations and several new simulations contribute to a model intercomparison exercise of three different contrail-cirrus models (Aktar-Martinez et al , in prep).

Improved VortexPhase Initialisation (VP-Init)

Further contrail vortex phase simulations with more realistic flow field initialisations (e.g. denoted as 'CFDInit' in Fig. 2, see also Pauen et al, 2024) have been performed, however, not all planned simulations of this block could be finished.

GEESE-VP and GEESE-DP

Formation flight scenarios of the contrail vortex phase (GEESE-VP) and the subsequent contrail-to-cirrus transition (GEESE-DP; DP = dispersion phase) have been investigated. The aim of GEESE-DP simulations is the quantification of saturation effects. Saturation means that the radiative effect of contrail-cirrus from an aircraft formation is smaller than that of the same number of aircraft flying in single missions. In analogy to a plot shown in Unterstrasser (2020), Fig. 2 bottom shows the radiative effect of contrail-cirrus from a single aircraft and formations with 2 or 3 aircraft. It demonstrates that the contrail-cirrus effect of the formations is for most atmospheric scenarios only slightly larger than a contrail produced by a single aircraft. Hence, formation flight is a promising contrail mitigation measure. Compared to the 2020 plot version, the vortex phase simulations are now based on a more realistic flow field initialisation. Moreover, formation scenarios with 3 aircraft have been investigated for the first time. The top row of Fig. 2 shows as an example how the contrail-cirrus radiative effect depends on the horizontal offset (DX) of two aircraft in formation. The simulation work is on-going and the robustness of the results will be further explored by analysing further atmospheric scenarios.

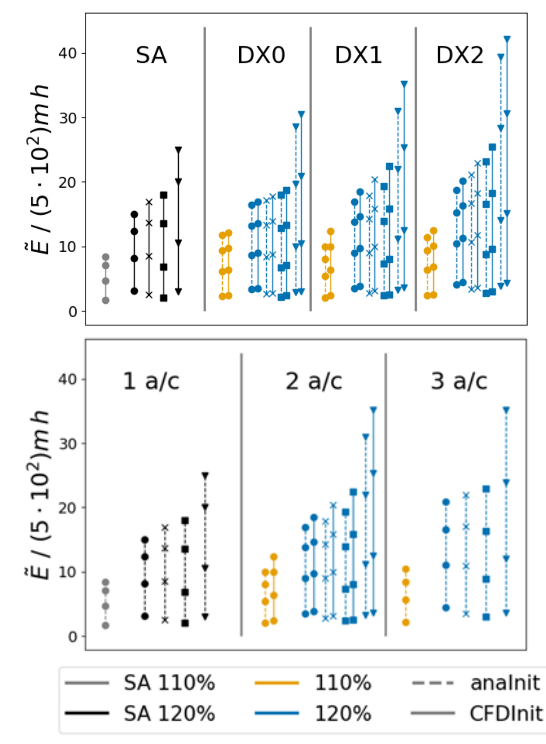

Figure 2: Contrail-cirrus saturation effects for single aircraft missions and aircraft formations with two or three participating aircraft (bottom row). The top row shows the sensitivity of the contrail-cirrus effect to the formation geometry (i.e. the relative position of two aircraft in a formation) Each data curve represents one simulation setup with corresponding VP and DP simulations.

REFERENCES

*In **bold** current and former members of DKRZ project 0832.*

Bier, A., Unterstrasser, S., Zink, J., Hillenbrand, D., Jurkat-Witschas, T., and **Lottermoser, A.:** Contrail formation on ambient aerosol particles for aircraft with hydrogen combustion: A box model trajectory study, Atmos. Chem. Phys., 24, 2319–2344, 2024

Lottermoser, A. and **Unterstrasser, S.:** High-resolution modelling of early contrail evolution from hydrogen-powered aircraft, ACP, 2025a, Article link

Lottermoser, A. and **Unterstrasser, S.:** Modeling the impact of alternative fuels and hydrogen propulsion on contrail-cirrus: a parameter study, in rev. for JGR, 2025b, Article link

Pauen, J., Unterstrasser, S. and Stephan, A.: Towards refined contrail simulations of formation flight scenarios, ICAS conference paper, ICAS2024_0502, p1-16, 2024, Article link

Akhtar Martínez C., **Lottermoser A., Unterstrasser S**., Eastham S. D., Jarrett J. P.: Intercomparison of contrail-cirrus simulations from three established models, in prep. for ACP